



## BIDIRECTIONAL GROUND MOTION EFFECTS IN TALL BUILDINGS USING 3D SOIL-STRUCTURE INTERACTION MODELS

L. G. Arboleda-Monsalve<sup>(1)</sup>, J. A. Mercado<sup>(2)</sup>, K. R. Mackie<sup>(3)</sup>

<sup>(1)</sup> Assistant Professor, Dept. of Civil, Environmental, and Construction Engineering, Univ. of Central Florida, Orlando, FL, 32816, USA. E-mail: [luis.arboleda@ucf.edu](mailto:luis.arboleda@ucf.edu)

<sup>(2)</sup> Research Assistant, Dept. of Civil, Environmental, and Construction Engineering, Univ. of Central Florida, Orlando, FL, 32816, USA. E-mail: [jamercado@knights.ucf.edu](mailto:jamercado@knights.ucf.edu)

<sup>(3)</sup> Professor, Dept. of Civil, Environmental, and Construction Engineering, Univ. of Central Florida, Orlando, FL, 32816, USA. E-mail: [Kevin.Mackie@ucf.edu](mailto:Kevin.Mackie@ucf.edu)

### Abstract

Numerical simulations of structures that consider soil-structure interaction (SSI) are usually performed under plane-strain conditions. Three-dimensional (3D) models are less common in the technical literature because of the computational time and storage required. In several numerical finite element platforms, advanced constitutive soil models are not coded yet for 3D applications or even for axisymmetric conditions. In a horizontal plane, earthquakes generally exhibit arbitrary principal directions of excitation that do not always coincide with the principal axes of the structure. The bidirectional nature of seismic wave fronts of most earthquakes modifies the structural seismic responses and trigger large structural demands in cases where the components of ground motion have correlated peaks. The main objective of the paper is to determine whether 3D numerical simulations including SSI effects amplify the bidirectional demands of tall buildings compared to more common fixed-base 3D analyses. In this paper, bidirectional ground motion effects on the seismic performance of tall buildings are included in 3D analyses using OpenSees by applying ground motions in two directions. Amplification or deamplification of engineering demand parameters are assessed due to the inclusion of SSI effects in relation to fixed-base 3D structural models. Supporting soils are modeled by means of a direct approach in a fully-coupled continuum soil-structure system formulation to represent in a more realistic manner the SSI effects. It is concluded that including bidirectional ground motion effects in tall buildings with SSI increase the engineering demand parameters when compared to fixed-base models. More realistic computation of seismic performance of tall buildings is achieved when bidirectional ground motions are applied at the base of a three-dimensional SSI model.

*Keywords: Bidirectional effects, 3D analysis, Soil-Structure Interaction (SSI); Tall Buildings; Direct Approach.*



## 1. Introduction

Modeling soil-structure interaction when analyzing the dynamic response of tall buildings, largely affects the dynamic characteristics of supporting soils and structure since the system is placed on a flexible support system that causes variations in the engineering demands parameters (EDPs) in relation to conventional fixed-base building models. Stewart et al. [1], Trifunac et al. [2,3], Tileylioglu [4], Givens [5], Karimi and Dashti [6], Tomeo et al. [7], Mercado and Arboleda-Monsalve [8], Arboleda-Monsalve et al. [9], among others, evaluated the contribution of SSI effects to the dynamic response of low-rise and tall buildings and concluded that SSI affects the distribution of EDPs in the structure. They concluded that oversimplified fixed-base assumptions are not always conservative. In the direct SSI modeling approach, the structure, foundation, and supporting soils are represented as a fully coupled system, in which the soil is modeled as a continuum [10]. The main limitations of two-dimensional (2D) modeling approaches from the structural point of view is that torsion and eccentricity effects of the building cannot be studied. Torsion on a building with irregularities may lead to large drift demands and therefore higher potential seismic-induced losses. From the soil modeling perspective, drainage patterns, which are three-dimensional in nature, are not readily captured. Also, Fu et al [11] stated that 2D models may overestimate the overall damping when compared to 3D models.. 3D SSI models are less common in the technical literature because of the computational time and storage required. Numerical simulations presented in this paper are developed assuming 3D conditions in the soil and structure using a direct approach to supersede some of the abovementioned limitations of 2D models.

This paper focuses on investigating numerically the interaction between a tall building and its supporting foundation soils in a 3D model subjected to bidirectional ground motions. First, the behavior of linear systems is assessed using linear-elastic formulations for the structure and supporting soils. Then, nonlinearities are included in the structural model to identify how SSI affects the seismic performance of tall buildings. Modification of the dynamic response of the structure by considering SSI is studied by computing EDP profiles which are compared to idealized fixed-base modeling conditions. Four numerical models are presented to assess the interaction between structure-soil systems when subjected to bidirectional seismic excitations. To accomplish this goal, two hypothetical 30-story tall building models were developed in OpenSees [12]: one building using linear-elastic structural elements and a second building using nonlinear elasto-plastic link elements to account for structural nonlinearities. Building stiffness and mass profiles were algorithmically generated to satisfy prescribed modes and reach target natural periods of the buildings of 4.0 and 3.5 s, in  $x$  and  $z$  directions respectively. Supporting soils were modeled using linear elastic materials based on field testing results recollected in downtown Los Angeles and a generalized soil profile is presented based on field investigation records. One earthquake ground motion of wide-range predominant frequency content was selected to study the broadband content that influences the response of the hypothetical tall buildings. Roof displacement and rotation, story shear, peak story horizontal acceleration and inter-story drift were computed to assess model differences on the computed structural response.

## 2. Subsurface Conditions and Soil Modeling Characteristics

The subsurface soil stratigraphy used for the SSI evaluation, correspond to downtown Los Angeles, California, and were based on field exploration data such as standard penetration tests (SPT) and shear wave velocity soundings ( $V_s$ ). The collected information is publicly available in the GeoDOG online tool developed by the California Department of Transportation and was supplemented with geotechnical data for the construction of three underground train stations in downtown Los Angeles, California [13]. **Fig. 1** presents the summarized field investigation data used to identify the subsurface conditions up to 40 m under the ground surface and the 3D free-field model used in OpenSees. The approximate location of the water table was 10.5 m from the ground surface. The submerged alluvium layer has an average  $D_r$  larger than 80%; thus, soil liquefaction is not expected. The soil profile was modeled using a 3D fully-coupled finite element soil domain using *SSPbrickUP* hexahedral 3D elements, capable of simulating the dynamic response of solid-fluid fully-coupled materials based on the Biot [14] theory for porous media. The mesh was discretized to have 8 to 10 elements per wavelength to avoid numerical dispersion. The finer parts of the mesh were used for the soil clusters underneath



and surrounding the tall buildings for the SSI analyses. The size of the soil domain was chosen to avoid large boundary effects and minimize computational time.

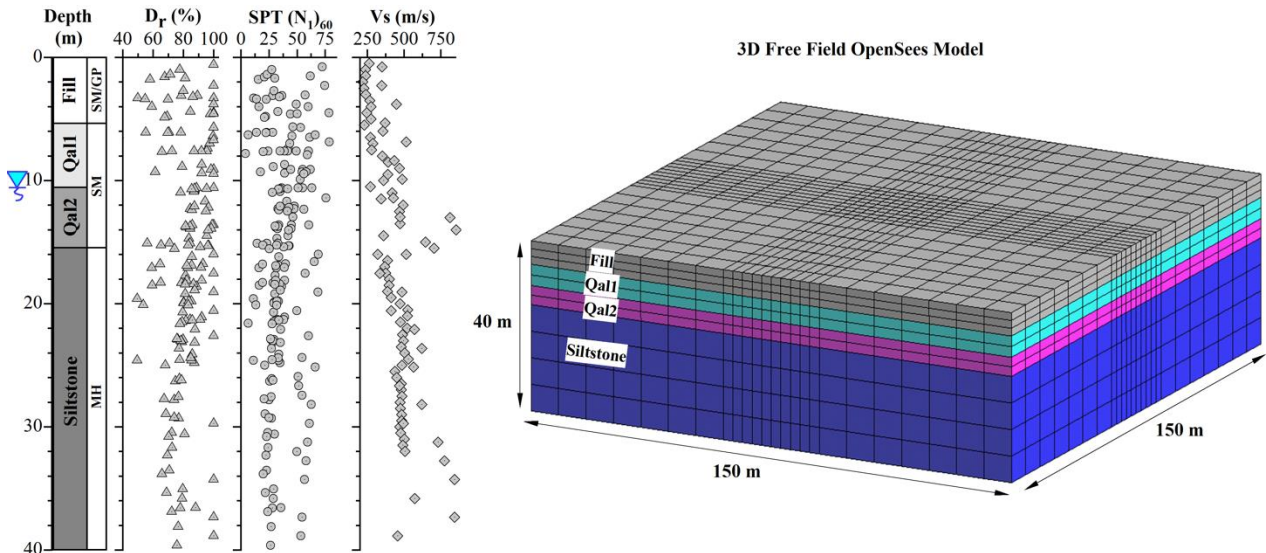


**Fig. 1 - Summarized subsurface conditions of downtown Los Angeles California and 3D free field OpenSees model.**

Elastic soil domain was assumed in the numerical simulations. The *ElasticIsotropic* model properties were derived from the geotechnical field test investigation program. Elastic material with large stiffness and weightless was also assigned to the soil domain to simulate a “firm” base condition so that fixed-base assumptions can also be studied for the proposed tall buildings. Table 1 presents the linear elastic soil parameters and their physical meaning. Poisson ratios ( $\nu$ ) were calculate based on the initial state of stresses of the soil. Elastic moduli ( $E$ ) were computed from the shear wave velocity investigation using classical relationships (i.e.,  $2G(1 + \nu)$  where  $G$  is the shear stress based on the  $V_s$  measurements). Supplemental 5% Rayleigh damping was included in the simulations to address the lack of material damping from the elastic soil.

**Table 1 - Soil parameters computed for the proposed soil conditions.**

Parameter	Description	Fill	Qal1	Qal2	Siltstone
$E$ (MPa)	Elastic modulus	332	497	1,050	1,570
$\nu$	Poisson ratio	0.34	0.30	0.32	0.33

### 3. Ground Motions

**Fig. 2a** shows the selected input ground motion for the analyses. The selected earthquake (EQ) was the Loma Prieta in 1989 recorded at station Sunnyvale-Colton Ave. (SVL) with a moment magnitude ( $M_w$ ) of 6.93. Components 270 and 360 were input in  $x$  and  $z$ -directions to account for bidirectional effects in the models. The recorded time histories were obtained using the PEER ground motion database tool (available at <https://ngawest2.berkeley.edu>). **Fig. 2b** presents the calculated Fourier amplitude using the Fast Fourier Transform (FFT) of each component of the ground motion time history. **Fig. 2c** shows the 5% damped pseudo spectral acceleration ( $S_a$ ) of each component of the SVL time history. The input time histories were scaled to match the spectral response acceleration ( $S_I$ ) of 0.4 g at a period of 1.0 s.

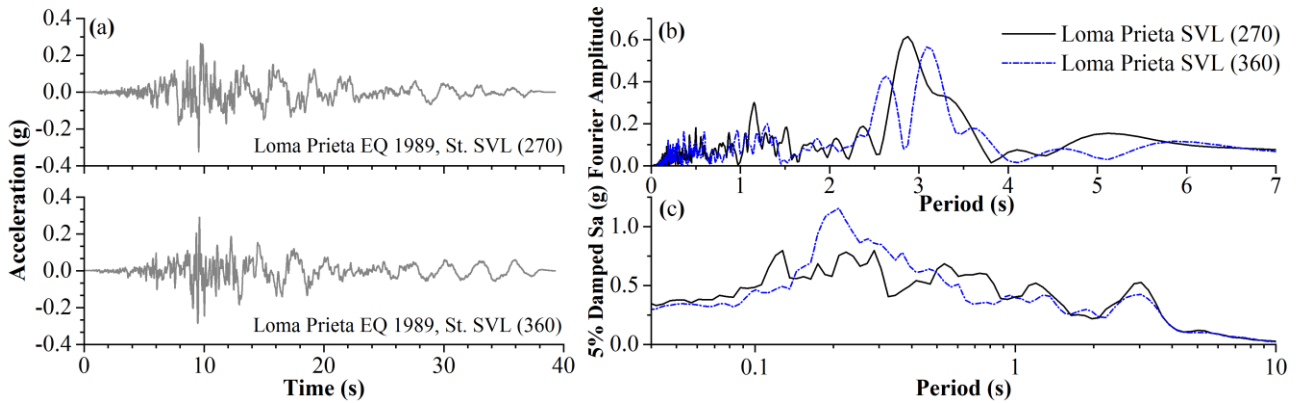


**Fig. 2 – SVL earthquake in both directions to analyze SSI effects: a) input acceleration time histories, b) Fourier amplitudes, and c) 5% damped spectral response accelerations.**

#### 4. Direct Soil-Structure-Interaction Modeling

**Fig. 3** presents the finite element 3D discretization of the SSI models developed in OpenSees. A supporting mat foundation with an approximate thickness of 1.8 m was modeled using brick elements with linear elastic concrete material properties. The bottom boundary of the soil domain was modeled assuming the nodes are fixed against displacements only in the vertical direction. On the sides, tied degrees of freedom (DOF) were applied to the nodes at the same elevation, therefore they had the same  $x$  and  $z$ -direction displacement. Periodic boundary conditions were assumed to represent a 1D analysis. At the bottom of the model, two Lysmer-Kuhlemeyer [30] dashpots were utilized in the  $x$  and  $z$  directions to account for the compliance of the underlying elastic medium. The dashpot properties were selected to represent the siltstone material found in the geotechnical field testing reports (i.e.,  $V_s = 700$  m/s and mass density of  $2.5$  Mg/m<sup>3</sup>). Ground motions were input to the model in terms of displacement time histories and using multiple-support excitations (i.e., *MultipleSupport* in OpenSees) The prescribed ground motions were input at the dashpots in the corresponding direction. As stated by Mercado et al. [15], the use of uniform excitation is not recommended for nonlinear systems when yielding occurs in the elements.

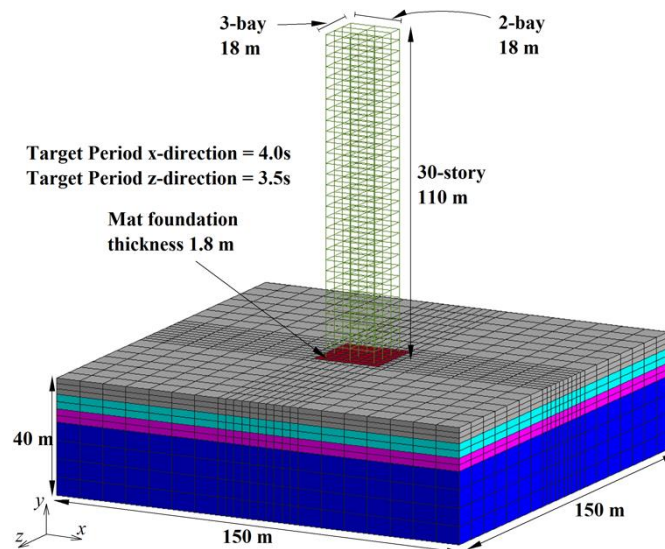


**Fig. 3 – 3D Soil-structure interaction finite element model of the tall buildings using direct approach.**

The tall building archetype has 30 stories, two bays in the  $x$ -direction and three bays in the  $z$ -direction (i.e., width of 18 m in each side of the building), and an approximate height of 110 m which represent an aspect



ratio of 8. Floors have all the same height (i.e., 3.67 m) except the bottom story that was selected to have a height of 4.1 m and a reduced stiffness to consider a soft story. Building properties were determined based on ASCE 7-16 [16] guidelines for steel moment-resisting frames (SMRF), assuming a response modification coefficient ( $R$ ), deflection amplification factor ( $C_d$ ), and 1 s spectral acceleration of 8, 5.5, and 0.4 g, respectively. The ratio beam-to-column stiffness ( $EI_b/EI_c$ ) was assumed to be 0.5 times the ratio of the summation of the lengths ( $L_{b,total}/L_{c,total}$ ) at each floor, causing the building seismic response to be controlled by a mixed flexural and shear-type lateral response [17]. A flexible diaphragm was modeled using shell elements and moment releases with a large elastic modulus. The result was similar to the rigid diaphragm constraint that enforces equal in-plane deformations for the floors, without the restriction on the single-point constraints for the master node. Columns were assigned an overstrength factor of 1.25 to account for strong-column-weak-beam design philosophy. The column stiffnesses in each lateral frame direction were assumed to vary quadratically. The stiffness at the top is one half the stiffness at the base and there is no change of stiffness between base and first floor. The out-of-plane stiffness and strength of the beams was assumed to be the same as the in-plane properties.

The realization of each archetype was generated by solving the eigenvalue problem with an assumed initial mass profile with total weight of  $110(n_{bx}+1)(n_{bz}+1)n$  (in kN), where  $n_b$  is the corresponding number of bays in each direction and  $n$  is the number of stories. Only a single lateral degree of freedom was used in each orthogonal direction (i.e., rigid diaphragm assumption), with the mass at each floor coupling the eigenvalue solution between the two orthogonal frames. The mass distribution was assigned such that the first three periods satisfied those prescribed for each building direction. The solution was obtained solving the eigenvalue problem using a Newton approach, supplemented with importance sampling around the solution to guarantee that all six periods were satisfied. A tall building archetype with target natural period of 4 s in  $x$ -direction and 3.5 s in  $z$ -direction were used in this paper.

The elastic building models were created in OpenSees using *elasticBeamColumn* elements for columns and girders with the story stiffness properties obtained from the symbolic solution of the eigenvalue problem. This stiffness, combined with the mass solution, produced the same natural periods than the symbolic eigenvalue problem. The nonlinear model was created in OpenSees using nonlinear link elements (i.e., *twoNodeLink* elements) to define the shear and moment nonlinear force-deformation relationships independently for the girders and columns. The material used to enable the nonlinear behavior is the Giuffre-Menegotto-Pinto uniaxial strain hardening material model *Steel02* [18]. This material has a bilinear backbone curve with post-yielding stiffness, and it is characterized by continuity in the tangent stiffness during loading and unloading. Four models were developed based on the abovementioned modeling assumptions. Two models correspond to a 30-story tall building using fixed-base conditions (i.e., M1 and M2), where M1 uses linear elastic elements and M2 corresponds to the nonlinear building. SSI was included using linear elastic soils with parameters computed from classical shear wave velocity relationships, M3 and M4, paired with a linear and nonlinear structure, respectively.

## 5. Bidirectional Analyses of Tall Buildings

The bidirectional ground motion effects in the tall building models were studied. **Fig. 4** shows the computed story shear in  $x$  and  $z$  directions at the base, 15<sup>th</sup> and 30<sup>th</sup> story of the tall buildings. These story shears were calculated using the element horizontal forces in the global system at the end of the elements. Note how the shear demands in the buildings are larger at base and middle of the building, especially for linear buildings when compared to the roof responses. Nonlinear buildings had smaller bidirectional story shear demands than the linear buildings (i.e., compare M2 and M4 to M1 and M3), since yielding occur in the lower stories and thus large forces were not propagated higher up in the structure. Inclusion of SSI in the models, largely affected the bidirectional effects in the tall buildings due to the additional seismic-induced rocking of the structure from the supporting soil. SSI effects modified the coupling behavior between both directions of the buildings, generally producing larger story shears in when compared to the fixed-base tall buildings.

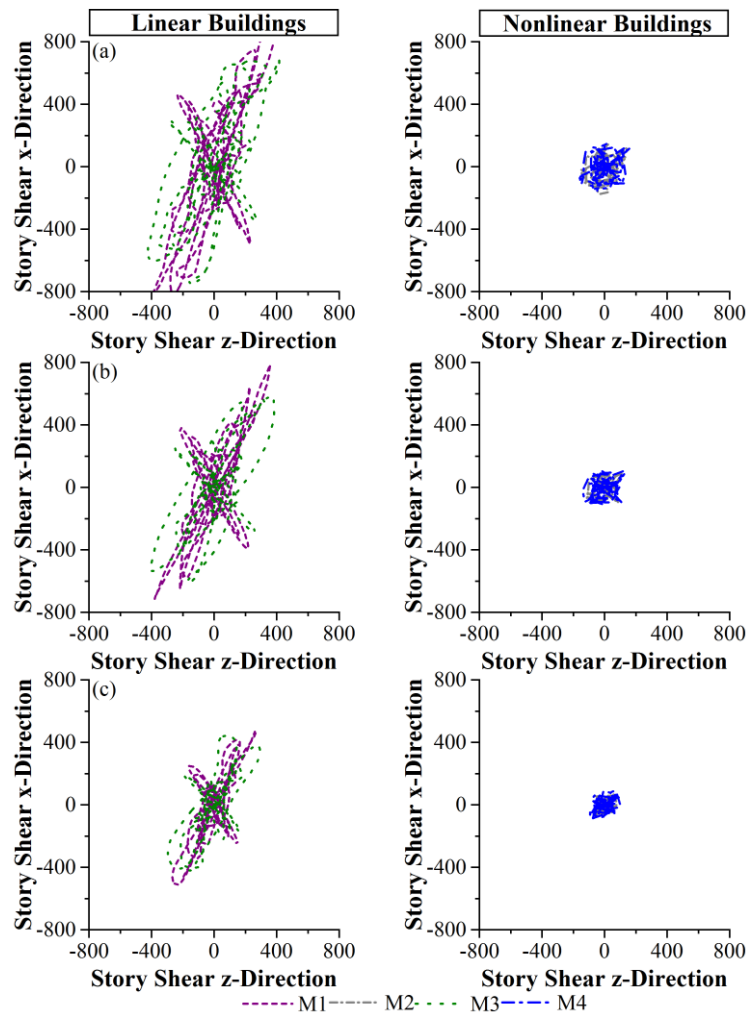


**Fig. 4 – Bidirectional story shear demands at: a) 1<sup>st</sup> story, b) 15<sup>th</sup> story, and c) 30<sup>th</sup> story.**

**Fig. 5** shows the computed inter-story drifts in  $x$  and  $z$  directions at the 30<sup>th</sup> story of the tall buildings. Nonlinear buildings had smaller bidirectional drift demands than the linear buildings (i.e., compare M2 and M4 to M1 and M3). Inclusion of SSI in the numerical models, affected the bidirectional drifts in the buildings by generally increasing the inter-story drift demands in both directions when compared to the fixed-base tall buildings (i.e., compare M3 to M1 and M4 to M2).

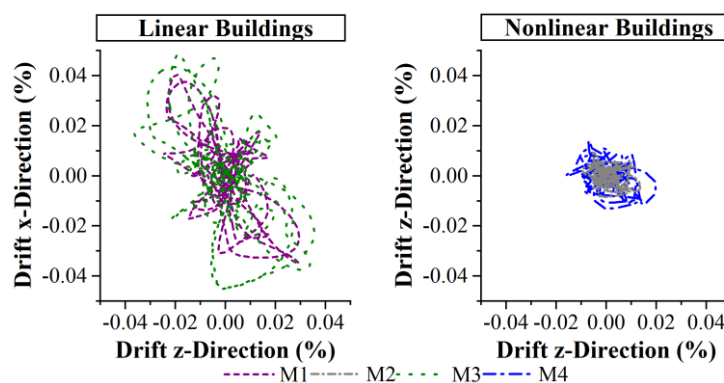


**Fig. 5 – Bidirectional inter-story drifts at the 30<sup>th</sup> story.**



**Fig. 6** shows the rotation time histories in degrees at the 30<sup>th</sup> story of the tall buildings. These rotations were computed based on  $x$  and  $z$ -direction movement of a corner column compared to the rigid diaphragm (i.e., to the middle of the floor plan). Note from the figure the rotation produced by the bidirectional effects included in the models with values up to 5°. Torsional effects seem plausible when modeling 3D tall buildings including SSI. Nonlinear structures tend to have smaller torsion than linear elastic tall buildings. Inclusion of SSI in tall buildings under bidirectional ground motion analyses increased the roof rotation.

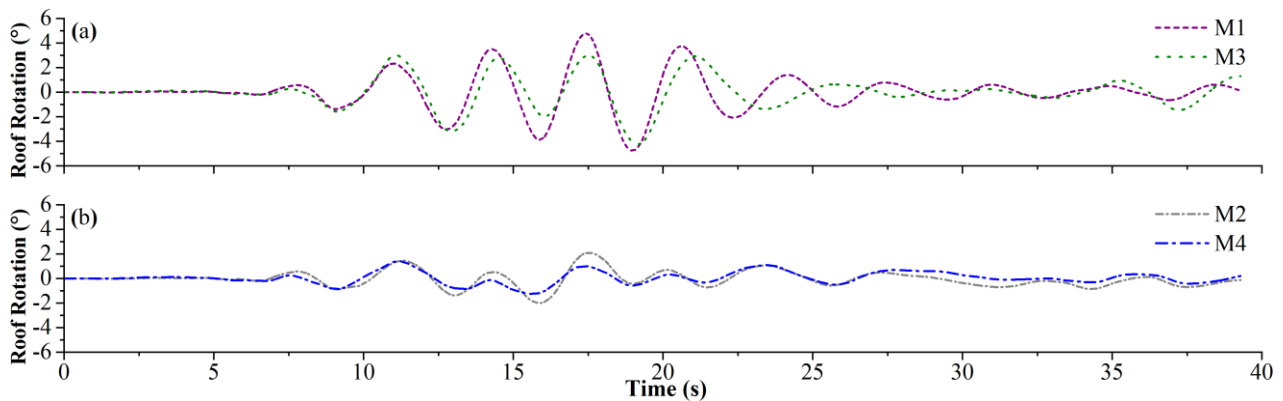


**Fig. 6** – Story rotation at the 30<sup>th</sup> story: a) linear elastic buildings and b) nonlinear buildings.

## 6. Peak Responses for the Tall Buildings

The EDPs considered in this paper are the peak horizontal accelerations and inter-story drifts. **Fig. 7a** presents the computed peak story horizontal accelerations for the models under each direction of the SVL earthquake. The accelerations presented in the figure are absolute. The differences in the acceleration demands between both directions are based on the natural period and the earthquake component used. In the  $z$ -direction, larger accelerations were computed than in  $x$ -direction. Recall that the target natural period in  $z$ -direction of the building is 3.5 s, which corresponded to a larger pseudo-acceleration than the 4 s in the  $x$ -direction in the forcing function spectrum. M1 and M3 buildings had larger horizontal acceleration than M2 and M4 buildings, since accelerations in the nonlinear buildings were propagated toward the top of the structure after yielding. Computed yielding was mainly concentrated at the base of the buildings. Note how SSI affects the peak acceleration profile in both directions. Generally, SSI increases the acceleration response in the tall buildings in both directions when compared to fixed-base models (i.e., compare SSI models M3 and M4 versus M1 and M2).

**Fig. 7b** presents the computed inter-story drifts for each direction of the SVL earthquake. Linear buildings produced larger inter-story drifts toward the top of the structure than nonlinear buildings (i.e., compare M2 and M4 versus M1 and M3). This is attributed to the material yielding in the lower stories in the nonlinear buildings. The directional effects are also shown in the figure, where the computed peak responses are larger in the  $z$ -direction of the building. SSI effects significantly altered the inter-story drift responses of the building due to the additional rocking arising from the flexible foundation soils. SSI effects with generally produced larger drift demands than the linear fixed-base buildings.

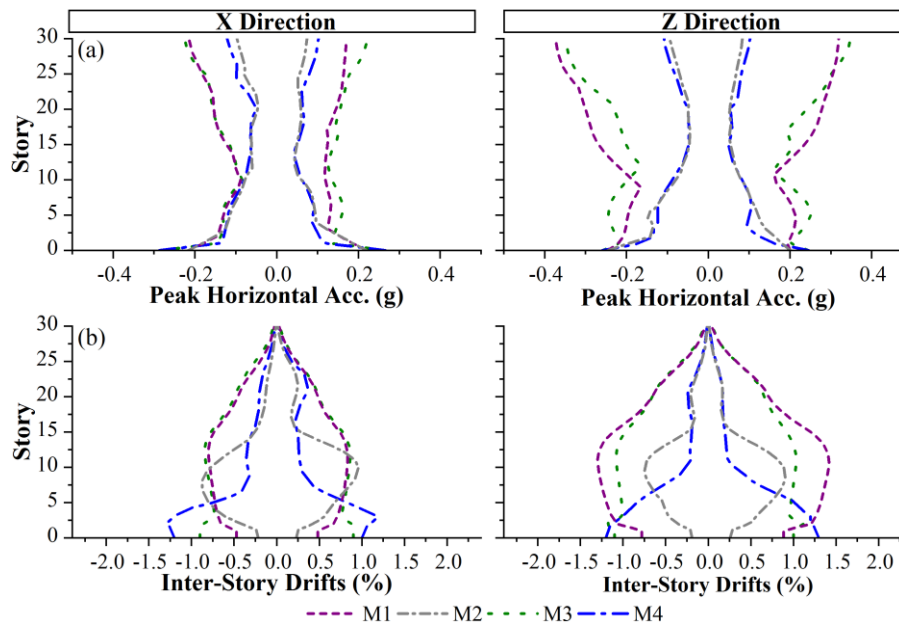


**Fig. 7 – Engineering demand parameter profiles in each direction for the tall buildings; a) peak horizontal accelerations and b) inter-story drifts.**

## 7. Summary and Conclusions

Nonlinear SSI effects on the seismic performance of tall buildings were investigated in this paper using numerical simulations. A total of four models were developed in OpenSees with different target periods (i.e., 4.0 and 3.5 s for  $x$  and  $z$  directions, respectively). Bidirectional effects were evaluated using story shears, roof displacements and rotations in both directions of the tall buildings. These bidirectional effects were highly influenced by the modeling assumptions, where for linear buildings larger demands were calculated in the tall buildings when compared to the nonlinear structures. SSI effects influenced the bidirectional effects by modifying the coupling behaviors between both directions of the buildings. Generally, larger bidirectional effects were computed in the SSI models compared to the fixed-base tall buildings. The roof rotation computation shows torsional effects during the earthquake in the tall buildings due to the modeling assumptions. Two EDPs were used to quantify the differences between models using profile responses: peak story horizontal accelerations and inter-story drifts. The results showed that fixed-base conditions are not always conservative and the inclusion of SSI effects in tall buildings affects the computed distribution of engineering demands along the structure height. Including bidirectional ground motion effects in tall buildings with SSI increase the engineering demand parameters when compared to fixed-base assumptions, which can lead to more realistic computation of seismic demands in current structural or geotechnical practice. Inclusion of SSI effects and the use of advanced 3D structural nonlinear models is strongly recommended by the authors when evaluating the seismic response of tall buildings.

## 8. Acknowledgements

Financial support for this work was provided by the National Science Foundation Grant No. CMMI-1563428. The support of Dr. Joy Pauschke and Dr. Richard Fragaszy, program directors at the National Science Foundation, is greatly appreciated.

## 9. References

- [1] Stewart JP., Fenves GL, Seed RB. (1999). Seismic Soil-Structure Interaction in Buildings. I: Analytical Methods. *J Geotech Geoenvironmental Eng* 125:26–37. [https://doi.org/10.1061/\(ASCE\)1090-](https://doi.org/10.1061/(ASCE)1090-)



0241(1999)125:1(26).

- [2] Trifunac MD, Ivanović SS, Todorovska MI. (2001). Apparent Periods of a Building. II: Time-Frequency Analysis. *J Struct Eng* 127:527–37. [https://doi.org/10.1061/\(ASCE\)0733-9445\(2001\)127:5\(527\)](https://doi.org/10.1061/(ASCE)0733-9445(2001)127:5(527)).
- [3] Trifunac MD, Ivanović SS, Todorovska MI. (2001). Apparent Periods of a Building. I: Fourier Analysis. *J Struct Eng* 127:517–26. [https://doi.org/10.1061/\(ASCE\)0733-9445\(2001\)127:5\(517\)](https://doi.org/10.1061/(ASCE)0733-9445(2001)127:5(517)).
- [4] Tileyliloglu S. (2008). Evaluation of Soil-Structure Interaction Effects from Field Performance Data. University of California, Los Angeles.
- [5] Givens MJ. (2013). Dynamic Soil-Structure Interaction of Instrumented Buildings and Test Structures. University of California, Los Angeles.
- [6] Karimi Z, Dashti S. (2016). Seismic Performance of Shallow Founded Structures on Liquefiable Ground: Validation of Numerical Simulations Using Centrifuge Experiments. *J Geotech Geoenvironmental Eng* 142:04016011. [https://doi.org/10.1061/\(ASCE\)GT.1943-5606.0001479](https://doi.org/10.1061/(ASCE)GT.1943-5606.0001479).
- [7] Tomeo R, Pitilakis D, Bilotta A, Nigro E. (2018). SSI effects on seismic demand of reinforced concrete moment resisting frames. *Eng Struct* 173:559–72. <https://doi.org/10.1016/j.engstruct.2018.06.104>.
- [8] Mercado JA, Arboleda-Monsalve LG. (2019). Influence of Substructure Levels on the Computed Seismic Performance of Low-Rise Structures. *J Earthq Eng*:1–17. <https://doi.org/10.1080/13632469.2019.1568928>.
- [9] Arboleda-Monsalve LG, Mercado JA, Terzic V, Mackie K. (2020). Soil-Structure Interaction Effects on Seismic Performance and Earthquake-Induced Losses in Tall Buildings. *J Geotech Geoenvironmental Eng*. [https://doi.org/10.1061/\(ASCE\)GT.1943-5606.0002248](https://doi.org/10.1061/(ASCE)GT.1943-5606.0002248).
- [10] National Institute of Standards and Technology NIST. (2012). Soil-Structure Interaction for Building Structures, Report NIST/GCR 12-917-21. vol. 12. <https://doi.org/12-917-21>.
- [11] Fu J, Todorovska MI, Liang J. (2018). Correction factors for SSI effects predicted by simplified models: 2D versus 3D rectangular embedded foundations. *Earthq Eng Struct Dyn* 47:1963–83. <https://doi.org/10.1002/eqe.3051>.
- [12] McKenna F, Fenves GL, Scott MH, Jeremic B. (2000). Open System for Earthquake Engineering Simulation (OpenSees).
- [13] AMEC. (2013). Final Geotechnical Data Report. Regional Connector Transit Corridor Project. Contract No. E0119. Prepared for Metro. Los Angeles, California: .
- [14] Biot MA. (1962). Generalized Theory of Acoustic Propagation in Porous Dissipative Media. *J Acoust Soc Am* 34:1254–64. <https://doi.org/10.1121/1.1918315>.
- [15] Mercado JA, Mackie KR, Arboleda-Monsalve LG. (2020). Nonlinear Soil-Structure Interaction Analyses of Tall Buildings. *Earthq Eng Struct Dyn*:Under Peer Review.
- [16] ASCE. (2017). Minimum Design Loads and Associated Criteria for Buildings and Other Structures. Reston, VA: American Society of Civil Engineers; . <https://doi.org/10.1061/9780784414248>.
- [17] Blume JA. (1968). Dynamic Characteristics of Multistory Buildings. *J Struct Div* 94:377–402.
- [18] Filippou FC, Popov EP, Bertero VV. (1983). Effects of Bond Deterioration on Hysteretic Behaviour of Reinforced Concrete Joints. Report to the National Science Foundation. *Earthq Eng Res Cent*:1–212.